Evolution and stability of ordered SiGe islands grown on patterned Si(100) substrates

C. Dais, G. Mussler, H. Sigg, E. Müller, H. H. Solak, and D. Grützmacher

Citation: Journal of Applied Physics **105**, 122405 (2009);
View online: https://doi.org/10.1063/1.3117230
View Table of Contents: http://aip.scitation.org/toc/jap/105/12
Published by the American Institute of Physics

Evolution and stability of ordered SiGe islands grown on patterned Si(100) substrates

C. Dais,[1,a)] G. Mussler,[2] H. Sigg,[1] E. Müller,[1,3] H. H. Solak,[1,4] and D. Grützmacher[2]
[1]*Laboratory for Micro- and Nanotechnology, Paul Scherrer Institute, Villigen 5232, Switzerland*
[2]*Institute of Bio-and Nanosystems, Research Center Jülich, Jülich 52425, Germany*
[3]*Electron Microscopy ETH Zürich (EMEZ), ETH-Zürich, Zürich 8093, Switzerland*
[4]*EULITHA AG, Villigen 5232, Switzerland*

(Received 13 October 2008; accepted 27 February 2009; published online 18 June 2009; publisher error corrected 23 June 2009)

SiGe quantum dots are proposed as building blocks for future Si device technology. However, in order to exploit the full potential of SiGe islands, it is necessary to control their positioning and size on a nanometer length. This is achieved by templated self-assembly, which combines substrate patterning and subsequent epitaxy. In this paper we report on the evolution of SiGe islands on patterned substrates under consideration of small template variations and postgrowth annealing. The impact of the structural variations on the optical properties of the islands is investigated by photoluminescence measurements. © *2009 American Institute of Physics*.
[DOI: 10.1063/1.3117230]

I. INTRODUCTION

Promising candidates for the introduction into mainstream technology are semiconductor quantum dots (QDs), which represent a solid state system with zero-dimensional carrier confinement and are therefore often referred as artificial atoms. Especially semiconductor QDs prepared from Si and Ge are of interest not only because of their compatibility to Si microelectronics but also because the SiGe material system is a relatively simple model system to understand the fundamental nucleation mechanism. The most common way to produce SiGe QDs is by strained layer epitaxy via the Stranski–Krastanow (SK) growth mode. The driving force of this growth mode is the lattice mismatch of 4.2% between Si and Ge to create self-assembled SiGe QDs on top of an initial two-dimensional wetting layer (WL). Such dislocation free SiGe QDs are in general randomly distributed on the surface and nucleate with a rather broad size distribution. Within the past years large efforts have been undertaken to study and categorize these structures.

However, it is evident that the applicability of most QD concepts is closely related with the ability to correlate them. For applications, in particular size uniformity and exact positioning of QDs are required.[1,2] A possible route to realize two-dimensional and long range ordered QD arrays is templated self-assembly. Templated self-assembly employs lithography to predefine the nucleation sites for the subsequent overgrowth of Ge. With this technique various one-dimensional and two-dimensional ordered SiGe QD arrays were fabricated on patterned Si substrates.[3–5] It is found that the ordering improves the size distribution of the dots since the deposited Ge atoms are equally divided on the patterned pits. Certainly, to achieve uniform dot arrays, it is always required to adjust the growth parameters in such a way that they match the pit parameters. For instance a larger pit periodicity may cause dot nucleation between the pits. Such undesired effects can be corrected by simultaneously increasing the growth temperature in order to extend the diffusion length of the Ge atoms.[6] In principle templated self-assembly allows the fabrication of uniform QD arrays with different periodicities, sizes, shapes,[7] as well as symmetries[8] of the SiGe islands. Stacking of Si/Ge layers allows even the realization of three-dimensional QD crystals.[9] In this context it is worth mentioning that dots grown on patterned substrates undergo the same shape transitions as on flat substrates.[7] However with the advantage (provided that correct template and growth parameters are used) that a monomodal size distribution is observed. This is contrary to flat substrates where normally a bimodal or even a trimodal distribution is found and a monomodal island distribution is only achieved under special growth conditions.

In this paper the evolution of SiGe QDs under consideration of small template variations is investigated. *In situ* postgrowth annealing was performed to analyze the stability of the QD arrays. The undertaken characterization comprises not only structural aspect but also optical properties of the nanostructures, as observed by photoluminescence (PL) measurements.

II. EXPERIMENT

The templated Si(100) substrates are prepared by extreme ultraviolet interference lithography (EUV-IL) using the XIL-beamline at the Swiss light source (SLS).[10,11] The EUV-IL technique is based on multiple beam interference of EUV light diffraction masks. Our EUV-IL setup has been proven to be capable of fabricating high resolution structures with excellent uniformity, which is a basic requirement for the fabrication of tailored QD arrays. For our experiments two-dimensional pit patterns with a periodicity of 90 nm $\times$ 100 nm were exposed on polymethyl methacrylate

[a)]Electronic mail: christian.dais@psi.ch. Tel.: +41 56 310 2580. Fax: +41 56 310 2646.

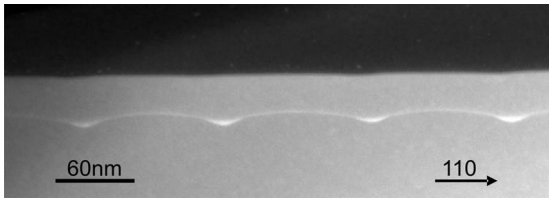

FIG. 1. Cross-sectional HAADF-STEM image of a nominal 2 ML thick Ge WL grown on pit patterned Si(100). The preferred Ge accumulation inside the pits results in periodic thickness variations of the WL.

(PMMA) coated Si(100) substrates. Subsequently, the PMMA is developed and the pattern is etched into Si by means of reactive ion etching using a mixture of CHF_3, SF_6, and O_2. After cleaning the substrates, they are transferred into a molecular beam epitaxy (MBE) chamber, equipped with electron-beam evaporators for the solid sources Si and Ge. First, the samples are only moderately annealed at 550 °C for 5 min to prevent smoothening—or even planarization—of the pits by thermally activated diffusion of Si atoms. Subsequently, a 50 nm thick Si buffer is grown at 410 °C, followed by Ge deposition of 2, 3, 5, and 7 ML while ramping the temperature from 410–580 °C. The samples for PL investigations are additionally capped with 40 nm of Si. Some of the samples are postgrowth annealed at 580 °C in the MBE system. Structural aspects were analyzed by means of scanning force microscopy (SFM) and high-angle annular dark field scanning transmission electron microscopy (HAADF-STEM). To investigate the optical properties of the QD arrays, PL measurements were performed using a Fourier transform infrared spectrometer equipped with a liquid-N_2-cooled InSb detector. For PL excitation the second harmonic of a yttrium aluminium garnet (YAG) laser at 532 nm is used. The large lateral extent of the patterned areas, which amounts to 770×700 μm^2 created with EUV-IL, allows a facile and exact alignment of the laser spot (diameter ~200 μm) on the patterned fields.

III. RESULTS AND DISCUSSION

A. Structural aspects

From a thermodynamic point of view the preferential nucleation at the bottom of the pits derives from capillarity effects, which are induced by a lowering of the chemical potential at the bottom of the pits.[12,13] Consequently, an increase of the growth rate at the pits bottoms occurs. This is already observable at the initial stage of SK growth during the WL formation. The STEM image in Fig. 1 is recorded from a sample with Ge coverage of 2 ML. Comparison measurements from a flat part of the sample indicate that this thickness is still below the critical thickness of island formation. This is also valid for the patterned area. In fact, the STEM gives already the impression that the patterned pits are preferred sites for Ge nucleation. In the patterned region the thickness of the WL is periodically modulated because of preferred Ge accumulation inside the pits.[14] Hence, the WL inside the pits is slightly thicker than the WL of the unpatterned region. However, the Ge accumulations have no characteristic dot facets and cannot be considered as full grown islands. For the employed growth parameters, the critical thickness of the unpatterned region is found at around 3 ML of Ge. At this value dot nucleation occurred already in each pit of the patterned area, which implies that the critical thickness of Ge coverage is reduced on patterned substrates as already reported in reference.[15]

Figures 2(b) and 2(c) depict QD arrays fabricated by 7 ML of Ge. The QD arrays differ only in the exposure dose, used for producing the EUV-IL patterns. Field A [Fig. 2(b)] is exposed with a lower dose compared to field B [Fig. 2(c)]. The different exposure doses influence the shape of the prepatterned pits, as can be seen in the profile plots in Fig. 2(a), which are measured before MBE deposition. An increase of pit width and depth is observed for field B due to the higher exposure dose. These variations in the pit geometry have strong impact on the uniformity of the QD arrays. The height dispersion of the islands in field A is considerably broader than in field B as shown in the distributions of Fig. 2(d). Recently, Zhong *et al.* studied the temperature dependence on SiGe islands grown on patterned substrates.[6] They found uniform dot formation only in a certain regime at intermediate temperature. Below and above this temperature, the dot uniformity degrades. Figure 2(c) demonstrates that the temperature in our experiments is chosen in this intermediate regime. However, our results imply that uniform dot formation exists only for certain pit morphology. It is assumed that the slightly shallower pits of the under exposed field promote Ostwald ripening, which is based on adatom diffusion between the islands and leads to the observed broader size distribution. Deeper pits work against Ostwald ripening since Ge has to be transported against the capillarity forces to a neighboring island. Hence, we conclude that well-defined and sufficient steep pits are mandatory for the formation of SiGe QDs with a uniform size distribution.

This conclusion is confirmed by the SFM images in Figs. 2(e) and 2(f). The presented dot arrays are identical to the samples depicted in Figs. 2(b) and 2(c) except that these samples have been *in situ* postgrowth annealed at 580 °C for 5 min inside the MBE chamber. The islands in field B [Fig. 2(f)] are still homogeneous and hence stable against annealing at this certain temperature. Only marginal size variations are observed by comparing the height distributions before and after annealing. This is not the case for the shallower pits of field A [Fig. 2(e)]. The size dispersion of this array has increased after annealing. The height distribution in Fig. 2(g) indicates that the larger dots grow at the expense of the smaller dots, which suggest a further ripening process due to annealing as typically observed for self-assembled dots grown on unpatterned substrates.[16] Obviously, the energy barrier for adatom diffusion created by the shallower pits of field A is not high enough to prevent adatom exchange between the pits.

B. Optical aspects

Figure 3 shows low temperature ($T=10$ K) PL spectra obtained from patterned and unpatterned areas. The dominant sharp line at 1095 meV observed in all spectra originates from the phonon-assisted replica (Si-TO) of the Si sub-

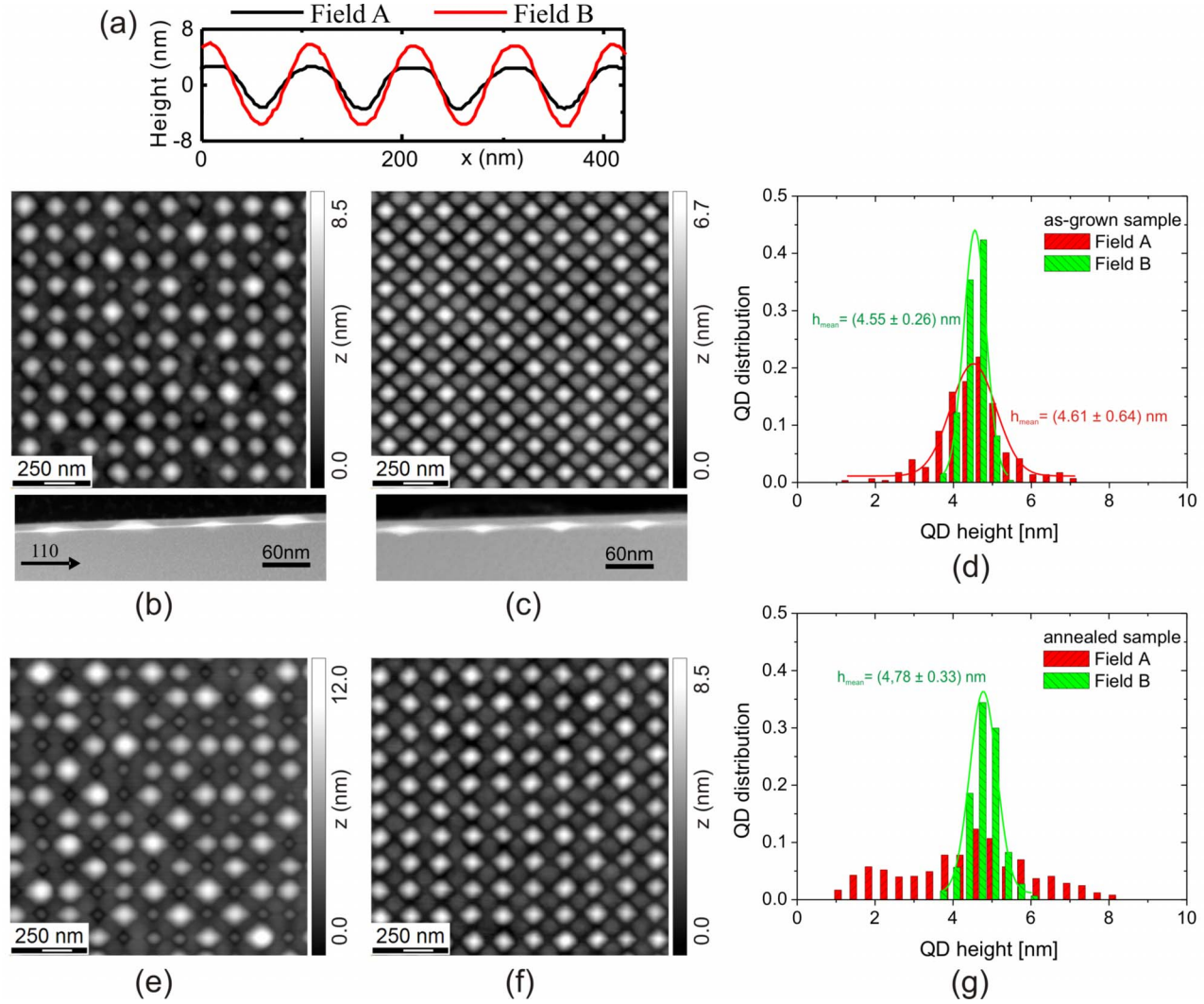

FIG. 2. (Color online) (a) Height profiles of the produced pit pattern. Field A is exposed with a lower EUV-IL exposure dose than field B. [(b) and (c)] SFM images (upper part) and cross-sectional HAADF-STEM images (lower part) of field A and B, respectively, after deposition of 7 ML Ge. [(e) and (f)] SFM images of field A and B after postgrowth annealing for 5 min at 580 °C.[(d) and (g)] Height distribution of the QD arrays before and after annealing, respectively.

strate and the Si epilayers. For a nominal Ge thickness of 2 ML, two additional lines at 1060 and 1002 meV are observable, which are attributed to the no-phonon (NP) and assisted transversal optical (TO) phonon of the pseudomorphic WL, respectively. Concerning the sample with 5 and 7 ML Ge, well-resolved double peak structures are observed for the patterned region. Deconvolution of this structure yield peaks at 952 meV (870 meV) and 903 meV (831 meV), which are attributed to the NP lines and assisted TO phonon lines of the 5 ML (7 ML) SiGe QDs. The associated linewidths amounts to 25 meV (32 meV) for the NP and 32 meV (41 meV) for the TO phonon peak. These remarkably small linewidths are a result of the narrow size distribution of the dots grown in patterned area. The redshift of the dot-related peaks from 5 to 7 ML structure is caused by an increase of the size and Ge concentration of the dots.

For comparison, the PL spectra obtained from the unpatterned area (7 ML of Ge) exhibit a much broader SiGe dot related PL signal due to the stronger size dispersion. Field A, which is exposed with a lower EUV-IL dose, represents an intermediate stage since the differences of the individual dots are not so pronounced as on the unpatterned area. In fact, NP and TO phonon peak are distinguishable but broader linewidths (NP line: 52 meV, TO phonon line: 62 meV) are obtained than for the uniform array in field B. The island-related PL peaks from field A and from the unpatterned region are redshifted compared to field B, again an effect of the broader size distribution. It is assumed that carriers are more likely captured from larger clusters, i.e., domes, observable in the nonuniform regions, which have a higher Ge concentration, lower bandgap, and lower confinement energies, resulting in the measured lower recombination energy.

The effect of postgrowth annealing on the optical properties is given in Figs. 3(f) and 3(g). First, let us consider the uniform dot region of field B. The dot related PL peaks shift slightly to higher energy (NP: 939 meV, TO: 889 meV), by maintaining the separation of NP and TO peak. The linewidths amounts to 31 meV for the NP line and to 43 meV for the TO phonon peak. Hence, we obtain similar values as for the as-grown sample, which corresponds to the similar size dispersion of the islands of field B before and after annealing [see Figs. 2(d) and 2(g)]. The observed blueshift is attributed

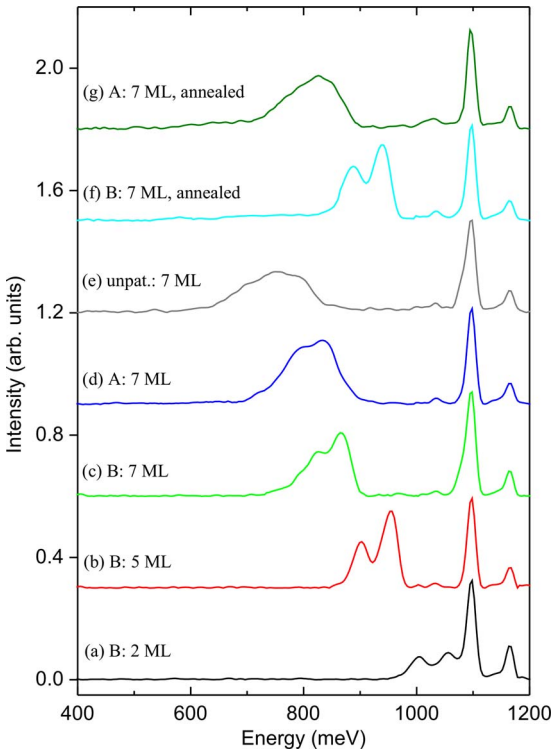

FIG. 3. (Color online) [(a)–(c)] 10 K PL spectra, measured in field B after deposition of 2, 5, and 7 ML Ge, respectively. [(d) and (e)] Corresponding 7 ML Ge PL spectra taken from field A and from nonpatterned region. [(f) and (g)] PL spectra of field B and A (7 ML Ge) after postgrowth annealing, respectively.

to enhanced Si/Ge intermixing during the long annealing step, as observed for dots grown on flat substrates.[17] Interestingly the TO phonon energy (energy difference between NP line and TO phonon line) increases from 39 meV for the as-grown sample to 50 meV for the annealed sample, which corresponds to a transition from a Ge–Ge TO phonon mode to a predominant Si–Ge TO phonon mode.[18] This observation is another indication for enhanced Si/Ge intermixing due to annealing, as the probability to create a Si–Ge TO phonon increases with lower Ge concentration.

The energy position of the PL signal of field A is almost stable after annealing. Certainly, intermixing should occur similarly or even stronger for this pattern since the material redistribution induced by annealing is enhanced compared to the uniform dot array. However, the observed ripening process results in larger dome clusters with respect to the sample without annealing. This contrary effect compensates the expected blueshift from intermixing and leads in total to the observed stable peak position. Besides, the PL signal broadens because of the wider size distribution after annealing.

IV. SUMMARY

In summary, we have observed the evolution of SiGe islands grown on EUV-IL patterned substrates. In particular, the dependence of array uniformity on the pit geometry was investigated. It was found that well-defined and steep holes are required to warrant the dot uniformity, which remains unaffected by postgrowth annealing. PL experiments on these structures demonstrate that the structural uniformity of the dots correlates to their optical properties, resulting in a narrow and stable PL emission.

ACKNOWLEDGMENTS

The authors thank A. Weber, S. Stutz, T. Neiger, and R. Schelldorfer for technical support and V. Auzelyte for EUV-IL mask preparation. This work is financially supported by the Swiss National Science Foundation. Part of the work was performed at the Swiss Light Source, Villigen, Switzerland.

[1] K. L. Wang, J. Nanosci. Nanotechnol. **2**, 235 (2002).
[2] O. G. Schmidt, A. Rastelli, G. S. Kar, R. Songmuang, S. Kiravittaya, M. Stoffel, U. Denker, S. Stufler, A. Zrenner, D. Grutzmacher, B. Y. Nguyen, and P. Wennekers, Physica E (Amsterdam) **25**, 280 (2004).
[3] Z. Y. Zhong, A. Halilovic, M. Muhlberger, F. Schaffler, and G. Bauer, J. Appl. Phys. **93**, 6258 (2003).
[4] Z. Y. Zhong, A. Halilovic, T. Fromherz, F. Schaffler, and G. Bauer, Appl. Phys. Lett. **82**, 4779 (2003).
[5] C. Dais, H. H. Solak, Y. Ekinci, E. Muller, H. Sigg, and D. Grutzmacher, Surf. Sci. **601**, 2787 (2007).
[6] Z. Zhong, P. Chen, Z. Jiang, and G. Bauer, Appl. Phys. Lett. **93**, 191101 (2008).
[7] J. J. Zhang, M. Stoffel, A. Rastelli, O. G. Schmidt, V. Jovanovic, L. K. Nanver, and G. Bauer, Appl. Phys. Lett. **91**, 3 (2007).
[8] C. Dais, H. H. Solak, E. Muller, and D. Grutzmacher, Appl. Phys. Lett. **92**, 143102 (2008).
[9] D. Grutzmacher, T. Fromherz, C. Dais, J. Stangl, E. Muller, Y. Ekinci, H. H. Solak, H. Sigg, R. T. Lechner, E. Wintersberger, S. Birner, V. Holy, and G. Bauer, Nano Lett. **7**, 3150 (2007).
[10] H. H. Solak, J. Phys. D **39**, R171 (2006).
[11] V. Auzelyte, C. Dais, P. Farquet, D. Grutzmacher, L. J. Heyderman, F. Luo, S. Olliges, C. Padeste, P. K. Sahoo, T. Thomson, A. Turchanin, C. David, and H. H. Solak, J. Micro/Nanolith. MEMS MOEMS **8**, 021204 (2009).
[12] M. Ozdemir and A. Zangwill, J. Vac. Sci. Technol. A **10**, 684 (1992).
[13] G. Biasiol, A. Gustafsson, K. Leifer, and E. Kapon, Phys. Rev. B **65**, 205306 (2002).
[14] A. Hartmann, C. Dieker, R. Loo, L. Vescan, H. Luth, and U. Bangert, Appl. Phys. Lett. **67**, 1888 (1995).
[15] Z. Y. Zhong, A. Halilovic, H. Lichtenberger, F. Schaffler, and G. Bauer, Physica E **23**, 243 (2004).
[16] T. I. Kamins, G. Medeiros-Ribeiro, D. A. A. Ohlberg, and R. S. Williams, J. Appl. Phys. **85**, 1159 (1999).
[17] M. W. Dashiell, U. Denker, C. Muller, G. Costantini, C. Manzano, K. Kern, and O. G. Schmidt, Appl. Phys. Lett. **80**, 1279 (2002).
[18] J. Weber and M. I. Alonso, Phys. Rev. B **40**, 5683 (1989).